

# Deeply virtual compton scattering at HERMES

YU Wei-Lin(俞伟林)<sup>1)</sup> (on behalf of the HERMES collaboration)

Physikalisches Institut, Justus-Liebig-Universität Gießen, Heinrich-Buff-Ring 16, 35392 Gießen, Germany

**Abstract** Generalized Parton Distributions (GPDs) provide a way to access total angular momenta of partons and give a multidimensional picture of the nucleon structure. Deeply Virtual Compton Scattering (DVCS) is the most direct exclusive process to study GPDs. Different azimuthal cross-section asymmetries with respect to beam helicity, beam charge, and target polarization have been measured in the HERMES experiment. A recoil detector was installed at HERMES to directly detect the recoil proton.

**Key words** compton scattering, QCD, nucleon structure

**PACS** 13.60.Fz, 12.38.-t, 14.20.Dh

## 1 Introduction

It was found from experiments that a large fraction of nucleon spin can not be completely explained by the intrinsic spin of quarks and gluons. Generalized Parton Distributions (GPDs) measured through the hard exclusive processes offer a possibility to determine orbital angular momenta of quarks. Deeply Virtual Compton Scattering (DVCS) is such a process that has been studied both theoretically and experimentally to further explore the nucleon spin structure. In the exclusive reaction the DVCS process interferes with the Bethe-Heitler (BH) process. This interference leads to various measurable azimuthal cross-section asymmetries. Different types of the azimuthal asymmetries give access to different GPDs.

## 2 GPDs and DVCS

In the hard exclusive process  $\gamma^*(q) + T(p) \rightarrow \gamma(q') + T'(p')$ , a virtual photon  $\gamma^*$  scatters off the hadronic target  $T$  and produces a real photon  $\gamma$  or a meson  $M$ , and a recoil state  $T'$ . It has been proven that such kind of reactions at high energy and large virtuality can be factorized into a perturbative and a non-perturbative parts. The perturbative part, corresponding to the interaction of a parton with a virtual photon, can be well calculated in perturbative QCD. The non-perturbative part, corresponding to the interaction of the scattered parton and the tar-

get nucleon, so far has not been calculated from first principles. In the light-cone framework this part can be parameterized by different GPDs.

At leading twist (twist-two), there are four quark helicity-conserving GPDs: the polarization-independent distributions  $H^q$  and  $E^q$  and the polarization-dependent distributions  $\tilde{H}^q$  and  $\tilde{E}^q$ . GPDs describe the multidimensional structure of the nucleon in terms of transverse spatial and longitudinal momentum distributions of partons. In addition, it has been proven that GPDs access the angular momentum of quarks by the second Mellin moments [1]:

$$\lim_{t \rightarrow 0} \int_{-1}^1 dx x (H^q(x, \xi) + E^q(x, \xi)) = 2J^q, \quad (1)$$

where  $J^q$  is the fraction of the nucleon angular momentum carried by a quark. This relation is also called Ji relation and holds for both, quarks and gluons. The Ji relation reveals the possibility to understand the composition of nucleon spin from quarks.

DVCS is the exclusive photon-production of a real photon, i.e.  $\gamma^*N \rightarrow \gamma N^*$ . It is theoretically the cleanest channel to study GPDs, however, experimentally it is impossible to distinguish the DVCS process from the elastic BH process, as both processes have the same initial and final states. The DVCS process generates a real photon by the interaction of a quark inside the nucleon while the BH process emits the photon by the incoming or outgoing electron. The total cross section of the two processes is proportional to

Received 26 January 2010

1) E-mail: yuwl@mail.desy.de

©2010 Chinese Physical Society and the Institute of High Energy Physics of the Chinese Academy of Sciences and the Institute of Modern Physics of the Chinese Academy of Sciences and IOP Publishing Ltd

the squared photon-production amplitudes written as

$$|T|^2 = |T_{\text{DVCS}}|^2 + |T_{\text{BH}}|^2 + T_{\text{DVCS}}T_{\text{BH}}^* + T_{\text{DVCS}}^*T_{\text{BH}}. \quad (2)$$

The two amplitudes  $T_{\text{DVCS}}$  and  $T_{\text{BH}}$  add coherently and thus lead to a interference term  $T_{\text{DVCS}}T_{\text{BH}}^* + T_{\text{DVCS}}^*T_{\text{BH}}$ , this interference term will be denoted as  $I$  in the rest of the text. Over the kinematics of the HERMES experiment, the BH process dominates the DVCS process. Fig. 1 shows the kinematics of real photon production in the target rest frame. The azimuthal angle  $\phi$  is the angle between the lepton scattering plane and the photon production plane, while  $\phi_S$  denotes the angle between the lepton plane and  $\vec{S}_\perp$ , the component of the target polarization vector for the case that target is transversely polarized.

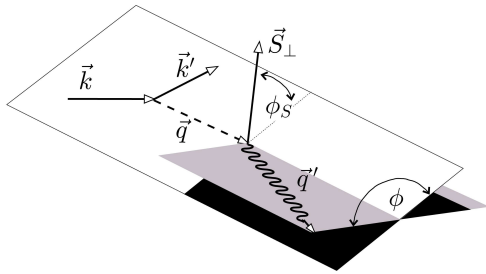


Fig. 1. (color online). Kinematics of real photon production in the target rest frame.

### 3 Azimuthal asymmetries

In order to extract information about the DVCS amplitudes from the measured azimuthal asymmetries, the amplitudes are expanded as a Fourier series. In the case of the unpolarized proton target, one obtains [2, 3]

$$|T_{\text{BH}}|^2 \propto \sum_{n=0}^2 c_n^{\text{BH}} \cos(n\phi), \quad (3)$$

$$|T_{\text{DVCS}}|^2 \propto \sum_{n=0}^2 c_n^{\text{DVCS}} \cos(n\phi) + \lambda s_1^{\text{DVCS}} \sin \phi, \quad (4)$$

and

$$I \propto e_i \left\{ \sum_{n=0}^3 c_n^I \cos(n\phi) + \sum_{n=1}^2 \lambda s_n^I \sin(n\phi) \right\}. \quad (5)$$

Here  $\lambda$  and  $e_i$  represent the beam helicity and beam charge respectively. Hence the coefficients  $s_1^{\text{DVCS}}$ ,  $c_n^I$  and  $s_n^I$  can be extracted by changing the beam charge and/or flipping the beam helicity. Theoretically it was revealed that the leading coefficients  $c_1^I$  and  $s_1^I$  provide access to the GPD  $H$  and thus are very important experimental observable. The other coeffi-

cients are either suppressed by higher twist or higher order of  $1/Q$  [4].

In the experiment  $s_1^I$  and  $s_1^{\text{DVCS}}$  can not be disentangled by flipping the beam helicity if only one beam-charge is available. The disentanglement can be achieved by looking at the charge-difference beam-helicity asymmetries when both beam-charges are available:

$$A_{\text{LU},I}(\phi) = \frac{(d\sigma^{++} - d\sigma^{+-}) - (d\sigma^{--} - d\sigma^{-+})}{(d\sigma^{++} + d\sigma^{+-}) + (d\sigma^{--} + d\sigma^{-+})} \\ \propto \sum_{n=1}^2 s_n^I \sin(n\phi), \quad (6)$$

and

$$A_{\text{LU,DVCS}}(\phi) = \frac{(d\sigma^{++} - d\sigma^{+-}) + (d\sigma^{--} - d\sigma^{-+})}{(d\sigma^{++} + d\sigma^{+-}) + (d\sigma^{--} + d\sigma^{-+})} \\ \propto s_1^{\text{DVCS}} \sin \phi. \quad (7)$$

While beam-charge asymmetry is

$$A_{\text{C}}(\phi) = \frac{d\sigma^+ - d\sigma^-}{d\sigma^+ + d\sigma^-} \propto \sum_{n=0}^2 c_n^I \cos(n\phi). \quad (8)$$

The above listed asymmetries can be simultaneously extracted by applying a maximum likelihood fit to the experimental yield  $\mathcal{N}$  according to the parameterization [3]:

$$\mathcal{N}(e_i, \lambda, \phi) = \mathcal{L}(e_i, \lambda) \eta(e_i, \phi) \sigma_{\text{UU}}(\phi) \times \\ [1 + \lambda A_{\text{LU,DVCS}}(\phi) + e_i \lambda A_{\text{LU},I}(\phi) + e_i A_{\text{C}}(\phi)]. \quad (9)$$

Here the Fourier coefficients can be expressed in terms of the asymmetry amplitudes, among which  $A_{\text{LU},I}^{\sin \phi}$  and  $A_{\text{C}}^{\cos \phi}$  are related to the leading coefficients  $s_1^I$  and  $c_1^I$ .  $\mathcal{L}$  and  $\eta$  denote the integrated luminosity and detection efficiency respectively.

The similar procedure was applied to the data of the transversely polarized proton target to extract the so-called transverse target-spin asymmetries through the corresponding Fourier coefficients [5]. Three leading asymmetry amplitudes  $A_{\text{UT},I}^{\cos(\phi - \phi_S) \sin \phi}$ ,  $A_{\text{UT},I}^{\sin(\phi - \phi_S) \cos \phi}$ , and  $A_{\text{UT,DVCS}}^{\sin(\phi - \phi_S)}$  are of great interest. They provide access to all four twist-two GPDs, especially to the GPD  $E$  which is an essential part to access the Ji relation.

### 4 The HERMES results

HERMES uses the 27.5 GeV longitudinal polarized electron/positron beam from HERA and polarized or unpolarized gas targets. For the DVCS studies, the cuts imposed on the electron/positron kinematics are:  $1 \text{ GeV}^2 < Q^2 < 10 \text{ GeV}^2$ ,  $0.03 < x_B < 0.35$ ,

and  $\nu < 22$  GeV. The real photon is required to deposit energy larger than 5 GeV in the calorimeter and larger than 1 MeV in the preshower detector.  $\theta_{\gamma^* \gamma}$ , the angle between the virtual and real photons is limited to a range from 5 to 45 mrad. The recoil proton was not detected in the data collected before 2006. Exclusive DVCS events were therefore selected by using the missing mass method. This was however limited by the relatively low detector resolutions and high background. The overall background is around 15% estimated by MC simulations, which is mainly due to the associated BH and semi-inclusive processes. The contribution from the associated BH process to the measured azimuthal asymmetries is still unclear, while the semi-inclusive contri-

bution was corrected by extracting asymmetries from  $\pi^0$  mesons [3, 5].

Fig. 2 shows the amplitudes of the beam-helicity asymmetry  $A_{LU,I}$  and  $A_{LU,DVCS}$  as a function of  $-t$ ,  $x_B$  and  $Q^2$ . The error bars (bands) represent the statistical (systematic) uncertainties. The systematic uncertainties are mainly due to possible misalignment of both beam and detectors, detector acceptance including smearing, finite bin width in the kinematics and correction of the semi-inclusive background. The two lines indicate the calculations based on two different GPD models [3]. While the fractional contribution of associated BH production is shown in the bottom row. The above mentioned five leading asymmetry amplitudes are listed in Table 1.

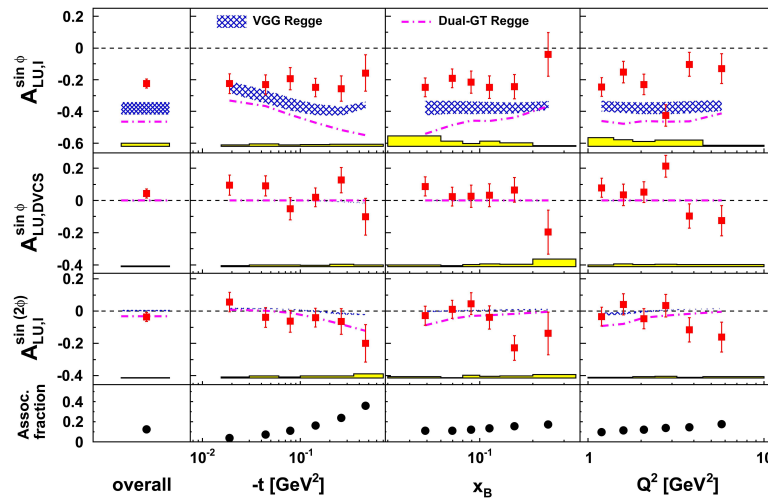


Fig. 2. (color online). Amplitudes of the beam-helicity asymmetry.

Table 1. Leading asymmetry amplitudes measured at HERMES.

Asymmetry amplitude	$\delta_{\text{stat}}$	$\delta_{\text{sys}}$
$A_{LU,I}^{\sin \phi}$	$-0.224$	$\pm 0.028$ $\pm 0.004$
$A_C^{\cos \phi}$	$0.055$	$\pm 0.028$ $\pm 0.004$
$A_{UT,I}^{\cos(\phi - \phi_s) \sin \phi}$	$0.005$	$\pm 0.040$ $\pm 0.015$
$A_{UT,I}^{\sin(\phi - \phi_s) \cos \phi}$	$-0.164$	$\pm 0.039$ $\pm 0.023$
$A_{UT,DVCS}^{\sin(\phi - \phi_s)}$	$-0.073$	$\pm 0.024$ $\pm 0.008$

Besides the asymmetries on unpolarized and transversely polarized proton targets, HERMES has

also carried out measurements of the asymmetries on longitudinally polarized proton target and on unpolarized nuclear targets. Furthermore, to improve the momentum resolution and to clean the background, a recoil detector was installed at HERMES in January 2006 to upgrade the detector performance by the ability to directly detect the recoil proton. The recoil detector was commissioned and took data with the forward spectrometer until the end of HERA running in June 2007. With the help of this unique set of data, HERMES will provide new insights into DVCS and GPDs.

## References

- 1 JI Xiang-Dong. Phys. Rev. Lett., 1997, **78**: 610–613; Phys. Rev. D, 1997, **55**: 7114–7125
- 2 Belitsky A V, Müller D, Kirchner A. Nucl. Phys. B, 2002, **629**: 323–392

- 3 Airapetian A et al (HERMES collaboration). JHEP, 2009, **11**: 083
- 4 Diehl M, Sapeta S. Eur. Phys. J. C, 2005, **41**: 515–533
- 5 Airapetian A et al (HERMES collaboration). JHEP, 2008, **06**: 066